

# UC Riverside

## UC Riverside Previously Published Works

### Title

Quantitative Assessment of Arsenite-Induced Perturbation of Ubiquitinated Proteome.

### Permalink

<https://escholarship.org/uc/item/7vp2s1b3>

### Journal

Chemical Research in Toxicology, 35(9)

### Authors

Jiang, Ji  
Wang, Yinsheng

### Publication Date

2022-09-19

### DOI

10.1021/acs.chemrestox.2c00197

Peer reviewed



# HHS Public Access

Author manuscript

*Chem Res Toxicol.* Author manuscript; available in PMC 2023 September 19.

Published in final edited form as:

*Chem Res Toxicol.* 2022 September 19; 35(9): 1589–1597. doi:10.1021/acs.chemrestox.2c00197.

## Quantitative Assessment of Arsenite-Induced Perturbation of Ubiquitinated Proteome

**Ji Jiang,**

Cell, Molecular, and Developmental Biology Graduate Program, University of California, Riverside, California 92521-0403, United States

**Yinsheng Wang**

Cell, Molecular, and Developmental Biology Graduate Program and Department of Chemistry, University of California, Riverside, California 92521-0403, United States

### Abstract

Arsenic contamination in food and groundwater constitutes a public health concern for more than 200 million people worldwide. Individuals chronically exposed to arsenic through drinking and ingestion exhibit a higher risk of developing cancers and cardiovascular diseases. Nevertheless, the underlying mechanisms of arsenic toxicity are not fully understood. Arsenite is known to bind to and deactivate RING finger E3 ubiquitin ligases; thus, we reason that a systematic interrogation about how arsenite exposure modulates global protein ubiquitination may reveal novel molecular targets for arsenic toxicity. By employing liquid chromatography-tandem mass spectrometry, in combination with stable isotope labeling by amino acids in cell culture (SILAC) and immunoprecipitation of di-glycine-conjugated lysine-containing tryptic peptides, we assessed the alterations in protein ubiquitination in GM00637 human skin fibroblast cells upon arsenite exposure at the entire proteome level. We observed that arsenite exposure led to altered ubiquitination of many proteins, where the alterations in a large majority of ubiquitination events are negatively correlated with changes in expression of the corresponding proteins, suggesting their modulation by the ubiquitin-proteasomal pathway. Moreover, we observed that arsenite exposure confers diminished ubiquitination of a rate-limiting enzyme in cholesterol biosynthesis, HMGCR, at Lys<sup>248</sup>. We also revealed that TRC8 is the major E3 ubiquitin ligase for HMGCR ubiquitination in HEK293T cells, and the arsenite-induced diminution of HMGCR ubiquitination is abrogated upon genetic depletion of TRC8. In summary, we systematically characterized arsenite-induced perturbations in a ubiquitinated proteome in human cells and found that the arsenite-elicited attenuation of HMGCR ubiquitination in HEK293T cells involves TRC8.

---

**Corresponding Author: Yinsheng Wang** – Cell, Molecular, and Developmental Biology Graduate Program and Department of Chemistry, University of California, Riverside, California 92521-0403, United States; Phone: (951) 827-2700; yinsheng.wang@ucr.edu; Fax: (951) 827-4713.

Complete contact information is available at: <https://pubs.acs.org/doi/10.1021/acs.chemrestox.2c00197>

Supporting Information

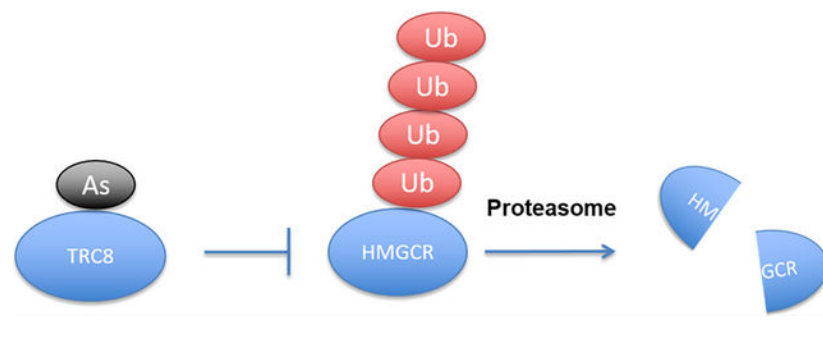
The Supporting Information is available free of charge at <https://pubs.acs.org/doi/10.1021/acs.chemrestox.2c00197>.

List of shRNA sequences used for knocking down the expression of genes encoding E3 ubiquitin ligases for HMGCR ubiquitination (PDF)

Detailed quantification data for ubiquitinated peptides in GM00637 cells with or without a 24 h treatment with 5  $\mu$ M NaAsO<sub>2</sub> (XLSX)

The authors declare no competing financial interest.

## Graphical Abstract



## INTRODUCTION

Being a metalloid, arsenic is ubiquitously present in soil and groundwater.<sup>1</sup> Arsenic species can be brought to the earth's surface through volcano eruption, rendering the surrounding environment rich in arsenic.<sup>2</sup> In water, inorganic arsenic species are dominant over organic arsenic species, and human exposure to inorganic arsenicals constitutes a major public health concern,<sup>3</sup> where arsenic exposure is strongly associated with the development of many human diseases, including cancer.<sup>4,5</sup>

The mechanisms of arsenic toxicity have caught researchers' attention for several decades. Recent studies revealed that As(III) is able to interact with cysteine sulfhydryl groups in zinc finger motifs of proteins, including RING finger-containing E3 ubiquitin ligases;<sup>6–16</sup> these latter interactions impair the capability of these ligases to ubiquitinate their substrate proteins.<sup>10–12,15–17</sup>

Ubiquitination represents one of the most important types of post-translational modifications in proteins and it plays significant roles in regulating protein–protein interactions, signal transduction, protein degradation, etc.<sup>18,19</sup> The ubiquitination process involves the conjugation of ubiquitin to the side chain of lysine residue(s) in substrate proteins, which is mediated by sequential actions of ubiquitin-activating enzymes (E1s), ubiquitin-conjugating enzymes (E2s), and ubiquitin ligases (E3s).<sup>18,19</sup> The 76-amino-acid protein ubiquitin itself can also be ubiquitinated on the N-terminus or one of its seven lysine residues, producing diverse polyubiquitin chains with complex topologies.<sup>20</sup>

Over the past several decades, researchers have used mass spectrometry in combination with other techniques to identify ubiquitination sites in proteins. In most cases, researchers ectopically overexpressed affinity-tagged ubiquitin in cells and immunoprecipitated ubiquitinated proteins for mass spectrometric analysis.<sup>21,22</sup> However, identification of ubiquitinated proteins with these methods is challenging owing to the low stoichiometry in protein ubiquitination. The disadvantages of these methods also arise from sample complexity, where both ubiquitinated and nonubiquitinated peptides are present in samples after proteolytic cleavage.<sup>23</sup> This may lead to a poor coverage of ubiquitinated peptides and a low signal-to-noise ratio for low-abundance ubiquitinated peptides because the samples are often overwhelmed with nonubiquitinated peptides. Therefore, comprehensive identification

of ubiquitination sites in the whole proteome entails selective enrichment of ubiquitinated peptides.

Substantial progress has been made toward the development of antibodies that specifically recognize the di-glycine remnant on lysine (i.e., K- $\epsilon$ -GG) generated from tryptic digestion of proteins harboring ubiquitinated lysine residues.<sup>24–27</sup> These peptides can be immunoprecipitated from trypsin digestion mixtures using the K- $\epsilon$ -GG antibodies, which enables the identification of ubiquitination sites in the whole proteome using LC-MS and MS/MS (Figure 1a).<sup>27,28</sup>

In the present study, we analyzed systematically the arsenite-elicited alterations in the ubiquitinated proteome of cultured human cells by using SILAC (stable isotope labeling by amino acids in cell culture)-based metabolic labeling,<sup>29</sup> immunoprecipitation with the K- $\epsilon$ -GG antibody, and LC-MS/MS analysis.<sup>27,28</sup> We were able to detect 1248 ubiquitination sites, among which the ubiquitination level of Lys<sup>248</sup> in HMGCR exhibited a fourfold diminution upon arsenite treatment. We also demonstrated that arsenite targets the TRC8 E3 ubiquitin ligase to inhibit HMGCR ubiquitination in HEK293T cells.

## EXPERIMENTAL SECTION

### Plasmid Construction.

Total RNA was extracted from HEK293T human embryonic kidney epithelial cells using the E.Z.N.A. Total RNA Kit I (Omega, Norcross, GA) and used as a template to construct the cDNA library by reverse transcription. The coding sequence of the *HMGCR* gene was PCR-amplified from the cDNA library and subsequently ligated into the *Bam*HI/*Xba*I sites of the pCDNA3.0 vector to yield the pCDNA3.0-HMGCR-Flag plasmid. The constructs were confirmed by Sanger sequencing. The plasmid for expressing HA-tagged ubiquitin was obtained from Addgene (Plasmid #18712).

The designed inserts for the construction of pLKO.1 vectors for the shRNA knockdown of *GP78*, *HRD1*, *MARCH6*, and *TRC8* genes were annealed, phosphorylated, and ligated to the dephosphorylated *Eco*RI/*Age*I sites of the pLKO.1 vector (Addgene, Plasmid #10878). The shRNA sequences are listed in Table S1, and the constructed plasmids were again validated by Sanger sequencing.

### Cell Culture and Transfection.

HEK293T and GM00637 cells were cultured in six-well plates in Dulbecco's modified Eagle medium (DMEM, ATCC, Manassas, VA) containing 10% fetal bovine serum (FBS, Invitrogen, Waltham, MA) and 100 U/mL penicillin and streptomycin, and the cells were maintained at 37 °C in a humidified cabinet containing 5% CO<sub>2</sub>. Typically, 1  $\mu$ g of the expression or shRNA plasmid was transfected into one well of cells with 5  $\mu$ L of Lipofectamine 2000 (Thermo Fisher, Waltham, MA).

### SILAC Labeling and As(III) Treatment.

GM00637 cells were cultured in a light or heavy RPMI 1640 medium. The heavy medium contained [<sup>13</sup>C<sub>6</sub>, <sup>15</sup>N<sub>2</sub>]-L-lysine (K8) and [<sup>13</sup>C<sub>6</sub>]-L-arginine (R6) instead of their unlabeled

counterparts. The cells were cultured in the heavy medium for at least 10 days, with a labeling efficiency of >95% as confirmed by LC-MS/MS analysis. The cells were then cultured for 24 h in the heavy medium containing 5  $\mu$ M As(III) or mock-treated in the light medium (forward SILAC), and vice versa (reverse SILAC), followed by a 1 h treatment with 5  $\mu$ M MG132. The light- and heavy-labeled cells were harvested and the whole-cell lysates were combined at a 1:1 ratio (by mass).

### Immunoprecipitation of Ubiquitin Remnant Peptides.

A mixture of 10 mg of the light and heavy protein lysates was reduced with dithiothreitol and alkylated with iodoacetamide, followed by an overnight digestion with trypsin at an enzyme/substrate mass ratio of 1:50. The tryptic peptides were subjected to a Sep-Pak C18 column (Waters) for sample desalting and purification, following published procedures.<sup>28</sup> The eluted peptides after desalting were subsequently incubated with the antibody provided in the PTMScan Ubiquitin Remnant Motif (K- $\epsilon$ -GG) Kit (Cell Signaling). The immunoprecipitated peptides were eluted with 0.15% trifluoroacetic acid, desalted with ZipTip (EMD Millipore), and subjected to LC-MS/MS analysis.

### LC-MS/MS Analysis of Ubiquitinated Peptides and Database Search.

The samples were analyzed on a Q-Exactive Plus Hybrid Quadrupole-Orbitrap mass spectrometer coupled with an EASY-nLC1200 (Thermo Fisher Scientific, San Jose, CA) in a data-dependent acquisition mode, where the 20 most abundant ions observed in MS were selected for MS/MS analyses. Mobile phases A and B contained 0.1% formic acid in water and 0.1% formic acid in acetonitrile, respectively. The flow rate was 230 nL/min, and the gradient included: 0 min, 0% B; 5 min, 9% B; 155 min, 39% B; 156 min, 88% B; 166 min, 95% B; and 181 min, 95% B.

Full-scan MS was acquired in the Orbitrap mass analyzer in the  $m/z$  range of 200–1200 with a resolution of 35 000 at  $m/z$  200. The twenty most abundant ions were fragmented in the HCD collision cell, and full-scan MS/MS were recorded in the Orbitrap mass analyzer with a resolution of 17 500 at  $m/z$  200. The maximum injection time for full-scan MS and MS/MS was 100 ms and 75 ms, respectively. The mass spectrometry proteomics data have been deposited to the ProteomeXchange Consortium via the PRIDE<sup>30</sup> partner repository with the dataset identifier PXD035401.

The raw LC-MS and MS/MS data were subjected to search using Maxquant<sup>31</sup> for protein identification against the FASTA human whole proteome database with a false discovery rate of 0.01. Trypsin was chosen as the digestion enzyme, where di-Gly modification on lysine and carbamidomethylation of cysteine were set as variable and fixed modifications, respectively. A cutoff ratio of 1.5 was imposed to consider a change in the peptide ubiquitination level to be substantial.

### Western Blot for Monitoring HMGCR Expression and Ubiquitination.

HEK293T cells were exposed to increasing concentrations of As(III) for 24 h. The cells were then harvested, lysed, and subjected to SDS-PAGE analysis. The proteins were subsequently transferred to a nitrocellulose membrane and probed for HMGCR and  $\beta$ -

actin, with the use of anti-HMGCR (1:5000) and anti-actin (1:10 000) (Abcam) primary antibodies, respectively.

In parallel, the cells were co-transfected with 1  $\mu\text{g}$  of HMGCR-Flag and 500 ng of HA-ubiquitin plasmids for 24 h and subsequently treated with 5  $\mu\text{M}$  As(III) for 24 h, followed by incubation with 5  $\mu\text{M}$  MG132 for 2 h. The cells were then lysed, and 80  $\mu\text{g}$  of the whole-cell lysate was incubated overnight with 30  $\mu\text{L}$  anti-Flag M2 magnetic beads (Thermo Fisher). After washing the beads with 1 $\times$  PBS three times, the bound proteins were eluted with 1 $\times$  SDS loading buffer at 95  $^{\circ}\text{C}$  for 5 min. The eluted proteins were subjected to SDS-PAGE separation and probed with the anti-HA (1:10 000) primary antibody to detect HMGCR ubiquitination.

## RESULTS

### Identification and Quantification of Ubiquitinated Peptides by LC-MS/MS.

We set out to investigate how arsenite exposure affects protein ubiquitination at the whole proteome level. Toward this end, we developed a workflow relying on SILAC-based metabolic labeling, enrichment of the ubiquitin remnant peptides by immunoprecipitation, and LC-MS/MS analysis. Briefly, we treated SILAC-labeled GM00637 cells with 5.0  $\mu\text{M}$  arsenite for 24 h, digested the whole-cell protein lysate with trypsin, and immunoprecipitated K- $\epsilon$ -GG-containing peptides from the tryptic digestion mixture. The samples were subsequently subjected to LC-MS/MS analysis in the data-dependent acquisition mode, and the raw data were searched against the FASTA human whole proteome database using Maxquant (Figure 1a). In this vein, U.S. Environmental Protection Agency set the maximum contaminant level of arsenic in public drinking water at 10 ppb ( $\sim$ 0.13  $\mu\text{M}$ ); however, the concentrations of arsenic in ground water in private wells in many areas of the U.S. and elsewhere in the world exceed that level.<sup>1</sup> In addition, humans are often exposed to arsenic-contaminated water for decades. To understand the molecular mechanisms through which arsenic exposure elicits adverse human health effects in a laboratory setting and to accommodate the needs of SILAC-based metabolic labeling, we chose to employ the above-mentioned treatment conditions.

The LC-MS/MS results led to the identification of 1248 K- $\epsilon$ -GG-containing peptides originating from 570 proteins and the quantification of 1086 site-specifically ubiquitinated peptides derived from 532 proteins. Among them, 193 ubiquitinated peptides from 130 proteins and 247 ubiquitinated peptides from 152 proteins were substantially down- and up-regulated (by at least 1.5-fold), respectively, upon a 24 h exposure to 5.0  $\mu\text{M}$  sodium arsenite, underscoring substantial alterations in the ubiquitinated proteome by arsenite exposure (Figure 1b). Figure 1c,d displays the quantification results for 25 proteins with the most pronounced decreases and increases, respectively, in ubiquitination levels after arsenite treatment. Among these proteins, the As(III)-induced diminution in monoubiquitination of endogenous FANCD2 was previously confirmed by Western blot analysis,<sup>11</sup> suggesting the robustness of the quantitative proteomic approach.

We previously examined, at the entire proteome scale, the alterations in expression of proteins in GM00637 cells under the same arsenite treatment conditions.<sup>32</sup> A correlation

analysis of the two datasets revealed that the fold changes in ubiquitination levels are negatively correlated with the fold changes in expression levels of the corresponding proteins (Figure 2), suggesting that a large fraction of ubiquitination events leads to proteasomal degradations of the corresponding proteins. Along this line, it is worth noting that our method, relying on analyzing K- $\epsilon$ -di-Gly remnant-containing peptides, cannot distinguish mono- from poly-ubiquitination or different topologies of ubiquitination from each other.

Since we are particularly interested in arsenite-mediated inhibition of ubiquitination, we conducted a KEGG pathway and functional category analyses for all of the 130 proteins from which the down-regulated ubiquitinated peptides were identified. These analyses revealed the role of arsenite in inducing diminished ubiquitination of proteins involved in the cholesterol synthesis pathway (Tables 1 and 2). In this vein, we identified six cholesterol synthesis-related proteins, including HMGCR, which is the rate-limiting enzyme in cholesterol biosynthesis (Table 2).<sup>33</sup>

### **Arsenite Exposure Leads to Diminished Ubiquitination and Proteasomal Degradation of HMGCR.**

We were also able to identify the Lys248-ubiquitinated peptide from HMGCR using LC-MS/MS analysis (Figure 3a,c). The relative abundance of this K- $\epsilon$ -GG-containing peptide was found to be decreased by ~73.4% upon a 24 h exposure of GM00637 cells to 5.0  $\mu$ M arsenite (Figure 3b). Hence, arsenite exposure confers a significantly attenuated ubiquitination of Lys248 in HMGCR, which is thought to be important for eliciting the proteasomal degradation of the protein.<sup>34</sup>

To substantiate the above finding, we also monitored the total ubiquitination level of HMGCR by using immunoprecipitation followed by Western blot analysis. To this end, we transfected HEK293T cells with plasmids for the ectopic expression of HMGCR-Flag and HA-ubiquitin and then treated the cells with different concentrations of arsenite. The cells were subsequently treated with MG132 to inhibit the proteasomal degradation of ubiquitinated proteins, and HMGCR-Flag was immunoprecipitated using anti-Flag M2 magnetic beads. The Western blot results showed that the levels of HMGCR ubiquitination exhibited a dose-dependent diminution upon arsenite treatment (Figure 4a).

It is well established that ubiquitination results in the proteasomal degradation of HMGCR.<sup>35</sup> Thus, we next explored if the arsenite-mediated inhibition of HMGCR ubiquitination gives rise to its stabilization. To this end, we measured basal levels of HMGCR proteins in HEK293T cells after exposure to different doses of arsenite (Figure 4b,c). The Western blot results showed a dose-dependent increase in the level of HMGCR proteins in cells, substantiating that the diminished ubiquitination of HMGCR by arsenite confers stabilization of the protein.

### **Arsenite Perturbs HMGCR Ubiquitination in HEK293T Cells through TRC8.**

Having demonstrated that arsenite negatively regulates the ubiquitination of HMGCR proteins in cells, we next explored the underlying mechanism. To this end, we first investigated which E3 ubiquitin ligase is responsible for HMGCR ubiquitination in

HEK293T cells. The level of HMGCR ubiquitination is tightly regulated under basal conditions, where ubiquitination serves as a signal for the proteasome-mediated degradation of HMGCR.<sup>36–39</sup> Several E3 ubiquitin ligases were previously documented to ubiquitinate HMGCR, including GP78, TRC8, MARCH6, and HRD1.<sup>36–39</sup> Thus, we examined the roles of these four E3 ubiquitin ligases in HMGCR ubiquitination in HEK293T cells by knocking down their expression levels using shRNAs and subsequently monitoring the ubiquitination level of HMGCR.

To better detect ubiquitination of HMGCR, we ectopically expressed Flag-tagged HMGCR and HA-tagged ubiquitin in HEK293T cells and treated the transfected cells with MG132 to stabilize ubiquitinated HMGCR. After immunoprecipitating HMGCR-Flag using anti-Flag M2 magnetic beads, we monitored HMGCR ubiquitination by Western blot analysis. In this vein, RT-qPCR results showed that the expression levels of all four E3 ligases were depleted by approximately 75% upon treatment with the corresponding shRNA (Figure 5a). We observed a significant decrease in HMGCR ubiquitination only upon knockdown of *TRC8*, but not any of the other three E3 ligase genes, underscoring that TRC8 constitutes the major E3 ubiquitin ligase for HMGCR ubiquitination in HEK293T cells (Figure 5b).

We next asked if TRC8 is responsible for the arsenite-mediated inhibition of HMGCR ubiquitination and degradation. Our results showed that the arsenite-elicited diminution in HMGCR ubiquitination was abrogated in HEK293T cells transfected with shTRC8, revealing the critical role of TRC8 in arsenite-mediated perturbation of HMGCR ubiquitination (Figure 5c).

## DISCUSSION

Human exposure to arsenic species through drinking water is a widespread public health concern, and exposure to arsenic is associated with the development of different human diseases, including cancer.<sup>4,5</sup> Several mechanistic models have been proposed for arsenic carcinogenesis,<sup>40</sup> among which the interaction between arsenic and cysteine residues in proteins has gained increasing attention in recent years.<sup>6,41</sup> Prior studies showed that the binding of As(III) to RING finger E3 ubiquitin ligases could compromise the ubiquitination of their substrate proteins.<sup>10–12,15–17</sup> There are many RING finger E3 ubiquitin ligases,<sup>42</sup> and it was unclear whether other E3 ligases are also targeted by As(III) and how such targeting modulates the ubiquitinated proteome in human cells.

LC-MS/MS analysis of K- $\epsilon$ -GG-containing peptides immunoprecipitated from the tryptic digestion mixture of the whole-cell protein lysate constitutes a robust and high-throughput workflow to assess the ubiquitin-modified proteome and to identify ubiquitination sites at the global proteome level.<sup>43</sup> Compared to other protein enrichment methods, the antibody-based enrichment of K- $\epsilon$ -GG-containing peptides helps reduce interferences from nonubiquitinated tryptic peptides, which allows for the identification of ubiquitinated peptides of low abundance. This workflow permits the establishment of ubiquitination networks in core signaling pathways and the identification of specific ubiquitination sites, thereby allowing for studying the functions of ubiquitination in a site-specific manner.<sup>24–27</sup>



In the present study, we applied this workflow to investigate the arsenite-mediated alterations of the ubiquitin-modified proteome. We were able to identify 1248 ubiquitinated peptides in GM00637 human skin fibroblasts (Figure 1); among them, the ubiquitination levels of 152 and 130 proteins were substantially up- and down-regulated, respectively, upon arsenite exposure. The fact that arsenite could both positively and negatively regulate the ubiquitination levels of different proteins reveals an intricate role of arsenite in modulating protein ubiquitination in cells. On the grounds that ubiquitination regulates various processes including protein–protein interactions, signal transduction, and protein degradation, these results suggest that arsenite may confer cytotoxicity and carcinogenicity partly through perturbing protein ubiquitination.

We conducted a functional annotation and pathway analysis using DAVID, which reveals that arsenite affects the ubiquitination levels of proteins involved in many important pathways. For instance, arsenite exposure resulted in altered ubiquitination levels of several proteins involved in DNA damage repair, including BRCA1, DDB1, FANCI, FANCD2, RAD23, and XRCC5 (Table S2). Along this line, our previous work showed that arsenite exposure compromises DNA interstrand cross-link repair through modulating FANCL-mediated FANCD2 monoubiquitination.<sup>11</sup> It will be important to examine, in the future, how arsenite exposure perturbs the ubiquitination of BRCA1, DDB1, RAD23, and XRCC5 and alters DNA repair pathways mediated by these protein factors.

We also identified diminished ubiquitination levels of six proteins that are associated with cholesterol biosynthesis, including HMGCR (Table 2). In particular, we were able to detect the K248- $\epsilon$ -GG-containing peptide of HMGCR by LC-MS/MS (Figure 3). In this context, it is worth noting that we also performed off-line SDS-PAGE fractionation of the whole-cell lysate and pull-down with an anti-Flag antibody to enrich ectopically expressed HMGCR-Flag proteins prior to tryptic digestion and LC-MS/MS analysis. We, however, failed to detect Lys248 ubiquitination in HMGCR with either approach, suggesting a low stoichiometry of this ubiquitination (data not shown) and the effectiveness of the antibody-based method in enriching K- $\epsilon$ -GG-containing peptides. This is not surprising viewing that this ubiquitination event leads to HMGCR degradation. In addition, we observed diminished ubiquitination of Lys248 in HMGCR upon arsenite treatment (Figure 3), indicating that arsenite may influence cholesterol synthesis by modulating HMGCR ubiquitination. Along this line, we found, from Western blot analysis, a dose-dependent attenuation in the total ubiquitination levels of HMGCR, which is accompanied by a concomitant elevation in the basal level of HMGCR upon arsenite treatment in HEK293T cells (Figure 4). These results suggest that the arsenite-induced suppression of HMGCR ubiquitination led to the stabilization of HMGCR proteins.

Cholesterol is an essential component of cell membranes, and it helps maintain membrane integrity and fluidity so as to enable animal cells to rapidly alter the shape in response to extracellular stimuli and intracellular cues.<sup>44</sup> Cholesterol is also a precursor for the biosynthesis of many important biomolecules, including vitamin D, bile acid, and steroid hormones.<sup>45–47</sup> Cholesterol is synthesized through the mevalonate pathway, where the HMGCR-catalyzed conversion of HMG-CoA to mevalonate is the rate-limiting step.<sup>48</sup> Therefore, the level of HMGCR in cells is tightly correlated with the biosynthesis of

cholesterol and nonsterol isoprenoids. Cells regulate cholesterol biosynthesis through a feedback mechanism, where the level of the rate-limiting enzyme, HMGCR, is negatively regulated by sterol, i.e., a high concentration of sterol promotes the ubiquitination and proteasomal degradation of HMGCR.<sup>49</sup> Several E3 ubiquitin ligases have been proposed to be involved in the ubiquitination of HMGCR in a cell type-specific manner, including GP78, TRC8, MARCH6, and HRD1. In the present study, we knocked down the four E3 ubiquitin ligases individually in HEK293T cells and found that the genetic depletion of TRC8, but not any of the other three E3 ubiquitin ligases, led to diminished ubiquitination of HMGCR, suggesting that TRC8 is the major E3 ubiquitin ligase for HMGCR ubiquitination in HEK293T cells (Figure 5a,b). We also observed that the arsenite-induced perturbation of HMGCR ubiquitination was abolished after knocking down TRC8 in HEK293T cells, supporting the notion that arsenite targets TRC8 to inhibit HMGCR ubiquitination and degradation (Figure 5c).

It is worth noting a limitation of our study. In particular, our quantitative proteomic data were acquired using GM00637 human skin fibroblast cells, and our subsequent follow-up experiments for HMGCR were conducted using HEK293T cells. We chose HEK293T cells for the latter part of the study because of the relatively high transfection efficiency and by extension relatively high shRNA knockdown efficiency for this cell line. Nevertheless, our previously published studies showed that the As(III)-induced perturbations in ubiquitinations of histone H2B, FANCD2, NRF2, and RPS10/20 were commonly observed in multiple cell lines, including GM00637 and HEK293T cells.<sup>11,12,15,16</sup> This is in keeping with the mechanism through which As(III) perturbs the ubiquitination of these proteins, i.e., via targeting their corresponding E3 ubiquitin ligases (RNF20/RNF40, FANCL, RBX1, and ZNF598).<sup>11,12,15,16</sup> However, we cannot formally exclude the possibility that the ubiquitination of HMGCR in GM00637 cells may involve E3 ubiquitin ligase(s) other than TRC8.

In summary, by using a SILAC- and LC-MS/MS-based quantitative proteomics workflow, coupled with K- $\epsilon$ -GG peptide immunoprecipitation, we assessed quantitatively the alterations in the ubiquitin-modified proteome elicited by arsenite exposure in cultured human cells, and we identified TRC8 as a new target for arsenite binding to inhibit HMGCR ubiquitination and degradation in HEK293T cells. The proteomic data developed in the current study also built a strong foundation for understanding how arsenite exposure alters other cellular pathways in cells.

## Supplementary Material

Refer to Web version on PubMed Central for supplementary material.

## ACKNOWLEDGMENTS

This work was supported by the National Institutes of Health (R35 ES031707).

## REFERENCES

- (1). Mukherjee A; Sengupta MK; Hossain MA; Ahamed S; Das B; Nayak B; Lodh D; Rahman MM; Chakraborti D Arsenic contamination in groundwater: a global perspective with emphasis on the Asian scenario. *J. Health Popul. Nutr* 2006, 24, 142–163. [PubMed: 17195556]
- (2). Campos VL; Escalante G; Yanez J; Zaror CA; Mondaca MA Isolation of arsenite-oxidizing bacteria from a natural biofilm associated to volcanic rocks of Atacama Desert, Chile. *J. Basic Microbiol* 2009, 49, S93–S97. [PubMed: 19718679]
- (3). Ramírez-Solís A; Mukopadhyay R; Rosen BP; Stemmler TL Experimental and theoretical characterization of arsenite in water: Insights into the coordination environment of As-O. *Inorg. Chem* 2004, 43, 2954–2959. [PubMed: 15106984]
- (4). Saint-Jacques N; Brown P; Nauta L; Boxall J; Parker L; Dummer TJB Estimating the risk of bladder and kidney cancer from exposure to low-levels of arsenic in drinking water, Nova Scotia, Canada. *Environ. Int* 2018, 110, 95–104. [PubMed: 29089168]
- (5). Chen CL; Chiou HY; Hsu LI; Hsueh YM; Wu MM; Wan YH; Chen CJ Arsenic in drinking water and risk of urinary tract cancer: A follow-up study from northeastern Taiwan. *Cancer Epidemiol., Biomarkers Prev* 2010, 19, 101–110. [PubMed: 20056628]
- (6). Shen S; Li XF; Cullen WR; Weinfeld M; Le XC Arsenic binding to proteins. *Chem. Rev* 2013, 113, 7769–7792. [PubMed: 23808632]
- (7). Qin XJ; Liu W; Li YN; Sun X; Hai CX; Hudson LG; Liu KJ Poly(ADP-ribose) polymerase-1 inhibition by arsenite promotes the survival of cells with unrepaired DNA lesions induced by UV exposure. *Toxicol. Sci* 2012, 127, 120–129. [PubMed: 22387748]
- (8). Sun X; Zhou X; Du L; Liu W; Liu Y; Hudson LG; Liu KJ Arsenite binding-induced zinc loss from PARP-1 is equivalent to zinc deficiency in reducing PARP-1 activity, leading to inhibition of DNA repair. *Toxicol. Appl. Pharmacol* 2014, 274, 313–318. [PubMed: 24275069]
- (9). Zhou X; Sun X; Cooper KL; Wang F; Liu KJ; Hudson LG Arsenite interacts selectively with zinc finger proteins containing C3H1 or C4 motifs. *J. Biol. Chem* 2011, 286, 22855–22863. [PubMed: 21550982]
- (10). Zhang XW; Yan XJ; Zhou ZR; Yang FF; Wu ZY; Sun HB; Liang WX; Song AX; Lallemand-Breitenbach V; Jeanne M; Zhang QY; Yang HY; Huang QH; Zhou GB; Tong JH; Zhang Y; Wu JH; Hu HY; de The H; Chen SJ; Chen Z Arsenic trioxide controls the fate of the PML-RAR $\alpha$  oncoprotein by directly binding PML. *Science* 2010, 328, 240–243. [PubMed: 20378816]
- (11). Jiang J; Bellani M; Li L; Wang P; Seidman MM; Wang Y Arsenite binds to the RING finger domain of FANCL E3 ubiquitin ligase and inhibits DNA interstrand crosslink repair. *ACS Chem. Biol* 2017, 12, 1858–1866. [PubMed: 28535027]
- (12). Jiang J; Tam LM; Wang P; Wang Y Arsenite targets the RING finger domain of Rbx1 E3 ubiquitin ligase to inhibit proteasome-mediated degradation of Nrf2. *Chem. Res. Toxicol* 2018, 31, 380–387. [PubMed: 29658272]
- (13). Tam LM; Jiang J; Wang PC; Li L; Miao WL; Dong XJ; Wang YS Arsenite binds to the zinc finger motif of TIP60 histone acetyltransferase and induces its degradation via the 26S proteasome. *Chem. Res. Toxicol* 2017, 30, 1685–1693. [PubMed: 28837777]
- (14). Liu S; Jiang J; Li L; Amato NJ; Wang Z; Wang YS Arsenite targets the zinc finger domains of Tet proteins and inhibits Tet-mediated oxidation of 5-methylcytosine. *Environ. Sci. Technol* 2015, 49, 11923–11931. [PubMed: 26355596]
- (15). Zhang F; Paramasivam M; Cai Q; Dai X; Wang P; Lin K; Song J; Seidman MM; Wang Y Arsenite binds to the RING finger domains of RNF20-RNF40 histone E3 ubiquitin ligase and inhibits DNA double-strand break repair. *J. Am. Chem. Soc* 2014, 136, 12884–12887. [PubMed: 25170678]
- (16). Tam LM; Jiang J; Wang P; Wang Y Arsenite binds to ZNF598 to perturb ribosome-associated protein quality control. *Chem. Res. Toxicol* 2020, 33, 1644–1652. [PubMed: 32324387]
- (17). Tam LM; Wang Y Arsenic exposure and compromised protein quality control. *Chem. Res. Toxicol* 2020, 33, 1594–1604. [PubMed: 32410444]
- (18). Hochstrasser M Ubiquitin-dependent protein degradation. *Annu. Rev. Genet* 1996, 30, 405–439. [PubMed: 8982460]

- (19). Voutsadakis IA The ubiquitin-proteasome system and signal transduction pathways regulating Epithelial Mesenchymal transition of cancer. *J. Biomed. Sci* 2012, 19, 67. [PubMed: 22827778]
- (20). Callis J The ubiquitination machinery of the ubiquitin system. *Arabidopsis Book* 2014, 12, No. e0174. [PubMed: 25320573]
- (21). Danielsen JM; Sylvestersen KB; Bekker-Jensen S; Szklarczyk D; Poulsen JW; Horn H; Jensen LJ; Mailand N; Nielsen ML Mass spectrometric analysis of lysine ubiquitylation reveals promiscuity at site level. *Mol. Cell. Proteomics* 2011, 10, No. M110 003590.
- (22). Kirkpatrick DS; Denison C; Gygi SP Weighing in on ubiquitin: the expanding role of mass-spectrometry-based proteomics. *Nat. Cell Biol* 2005, 7, 750–757. [PubMed: 16056266]
- (23). Huynh ML; Russell P; Walsh B Tryptic Digestion of In-Gel Proteins for Mass Spectrometry Analysis. In *Methods in Molecular Biology*; Springer, 2009; Vol. 519, pp 507–513. [PubMed: 19381606]
- (24). Udeshi ND; Mani DR; Eisenhaure T; Mertins P; Jaffe JD; Clauser KR; Hacoen N; Carr SA Methods for quantification of in vivo changes in protein ubiquitination following proteasome and deubiquitinase inhibition. *Mol. Cell. Proteomics* 2012, 11, 148–159. [PubMed: 22505724]
- (25). Udeshi ND; Svinkina T; Mertins P; Kuhn E; Mani DR; Qiao JW; Carr SA Refined Preparation and Use of Anti-diglycine Remnant (K-epsilon-GG) Antibody Enables Routine Quantification of 10,000s of Ubiquitination Sites in Single Proteomics Experiments. *Mol. Cell. Proteomics* 2013, 12, 825–831. [PubMed: 23266961]
- (26). Kim W; Bennett EJ; Huttlin EL; Guo A; Li J; Possemato A; Sowa ME; Rad R; Rush J; Comb MJ; Harper JW; Gygi SP Systematic and quantitative assessment of the ubiquitin-modified proteome. *Mol. Cell* 2011, 44, 325–340. [PubMed: 21906983]
- (27). Xu GQ; Paige JS; Jaffrey SR Global analysis of lysine ubiquitination by ubiquitin remnant immunoaffinity profiling. *Nat. Biotechnol* 2010, 28, 868–U154. [PubMed: 20639865]
- (28). Udeshi ND; Mertins P; Svinkina T; Carr SA Large-scale identification of ubiquitination sites by mass spectrometry. *Nat. Protoc* 2013, 8, 1950–1960. [PubMed: 24051958]
- (29). Ong SE; Blagoev B; Kratchmarova I; Kristensen DB; Steen H; Pandey A; Mann M Stable isotope labeling by amino acids in cell culture, SILAC, as a simple and accurate approach to expression proteomics. *Mol. Cell. Proteomics* 2002, 1, 376–386. [PubMed: 12118079]
- (30). Perez-Riverol Y; Bai J; Bandla C; Garcia-Seisdedos D; Hewapathirana S; Kamatchinathan S; Kundu DJ; Prakash A; Frericks-Zipper A; Eisenacher M; Walzer M; Wang S; Brazma A; Vizcaíno JA The PRIDE database resources in 2022: A Hub for mass spectrometry-based proteomics evidences. *Nucleic Acids Res.* 2022, 50, D543–D552. [PubMed: 34723319]
- (31). Cox J; Mann M MaxQuant enables high peptide identification rates, individualized p.p.b.-range mass accuracies and proteome-wide protein quantification. *Nat. Biotechnol* 2008, 26, 1367–1372. [PubMed: 19029910]
- (32). Zhang F; Xiao Y; Wang Y SILAC-based quantitative proteomic analysis unveils arsenite-induced perturbation of multiple pathways in human skin fibroblast cells. *Chem. Res. Toxicol* 2017, 30, 1006–1014. [PubMed: 28140569]
- (33). Cerqueira NMFS; Oliveira EF; Gesto DS; Santos-Martins D; Moreira C; Moorthy HN; Ramos MJ; Fernandes PA Cholesterol Biosynthesis: A Mechanistic Overview. *Biochemistry* 2016, 55, 5483–5506. [PubMed: 27604037]
- (34). Miao HH; Jiang W; Ge LA; Li BL; Song BL Tetra-glutamic acid residues adjacent to Lys248 in HMG-CoA reductase are critical for the ubiquitination mediated by gp78 and UBE2G2. *Acta Biochim. Biophys. Sin* 2010, 42, 303–310. [PubMed: 20458442]
- (35). Hwang S; Hartman IZ; Calhoun LN; Garland K; Young GA; Mitsche MA; McDonald J; Xu F; Engelking L; DeBose-Boyd RA Contribution of accelerated degradation to feedback regulation of 3-hydroxy-3-methylglutaryl coenzyme A reductase and cholesterol metabolism in the liver. *J. Biol. Chem* 2016, 291, 13479–13494. [PubMed: 27129778]
- (36). Jiang W; Song BL Ubiquitin ligases in cholesterol metabolism. *Diabetes Metab J* 2014, 38, 171–180. [PubMed: 25003069]
- (37). Loregger A; Cook EC; Nelson JK; Moeton M; Sharpe LJ; Engberg S; Karimova M; Lambert G; Brown AJ; Zelcer N A MARCH6 and IDOL E3 ubiquitin ligase circuit uncouples cholesterol

- synthesis from lipoprotein uptake in hepatocytes. *Mol. Cell Biol* 2016, 36, 285–294. [PubMed: 26527619]
- (38). Kikkert M; Doolman R; Dai M; Avner R; Hassink G; van Voorden S; Thanedar S; Roitelman J; Chau V; Wiertz E Human HRD1 is an E3 ubiquitin ligase involved in degradation of proteins from the endoplasmic reticulum. *J. Biol. Chem* 2004, 279, 3525–3534. [PubMed: 14593114]
- (39). Jo Y; Lee PCW; Sguigna PV; DeBose-Boyd RA Sterol-induced degradation of HMG CoA reductase depends on interplay of two Insigs and two ubiquitin ligases, gp78 and Trc8. *Proc. Natl. Acad. Sci. U.S.A* 2011, 108, 20503–20508. [PubMed: 22143767]
- (40). Kitchin KT Recent advances in arsenic carcinogenesis: Modes of action, animal model systems, and methylated arsenic metabolites. *Toxicol. Appl. Pharmacol* 2001, 172, 249–261. [PubMed: 11312654]
- (41). Tam LM; Price NE; Wang Y Molecular mechanisms of arsenic-induced disruption of DNA repair. *Chem. Res. Toxicol* 2020, 33, 709–726. [PubMed: 31986875]
- (42). Lipkowitz S; Weissman AM RINGs of good and evil: RING finger ubiquitin ligases at the crossroads of tumour suppression and oncogenesis. *Nat. Rev. Cancer* 2011, 11, 629–643. [PubMed: 21863050]
- (43). Udeshi ND; Mertins P; Svinkina T; Carr SA Large-scale identification of ubiquitination sites by mass spectrometry. *Nat. Protoc* 2013, 8, 1950–1960. [PubMed: 24051958]
- (44). Krause MR; Regen SL The structural role of cholesterol in cell membranes: From condensed bilayers to lipid rafts. *Acc. Chem. Res* 2014, 47, 3512–3521. [PubMed: 25310179]
- (45). Rosenheim O; Webster TA The relation of cholesterol to vitamin D. *Biochem. J* 1927, 21, 127–129. [PubMed: 16743796]
- (46). Javitt NB Bile-acid synthesis from cholesterol - regulatory and auxiliary pathways. *FASEB J.* 1994, 8, 1308–1311. [PubMed: 8001744]
- (47). Qamar A; Bhatt DL Effect of low cholesterol on steroid hormones and vitamin E levels just a theory or real concern? *Circ. Res* 2015, 117, 662–664. [PubMed: 26405182]
- (48). Buhaescu I; Izzedine H Mevalonate pathway: A review of clinical and therapeutical implications. *Clin. Biochem* 2007, 40, 575–584. [PubMed: 17467679]
- (49). Tsai YC; Leichner GS; Pearce MMP; Wilson GL; Wojcikiewicz RJH; Roitelman J; Weissman AM Differential regulation of HMG-CoA reductase and Insig-1 by enzymes of the ubiquitin-proteasome system. *Mol. Biol. Cell* 2012, 23, 4484–4494. [PubMed: 23087214]

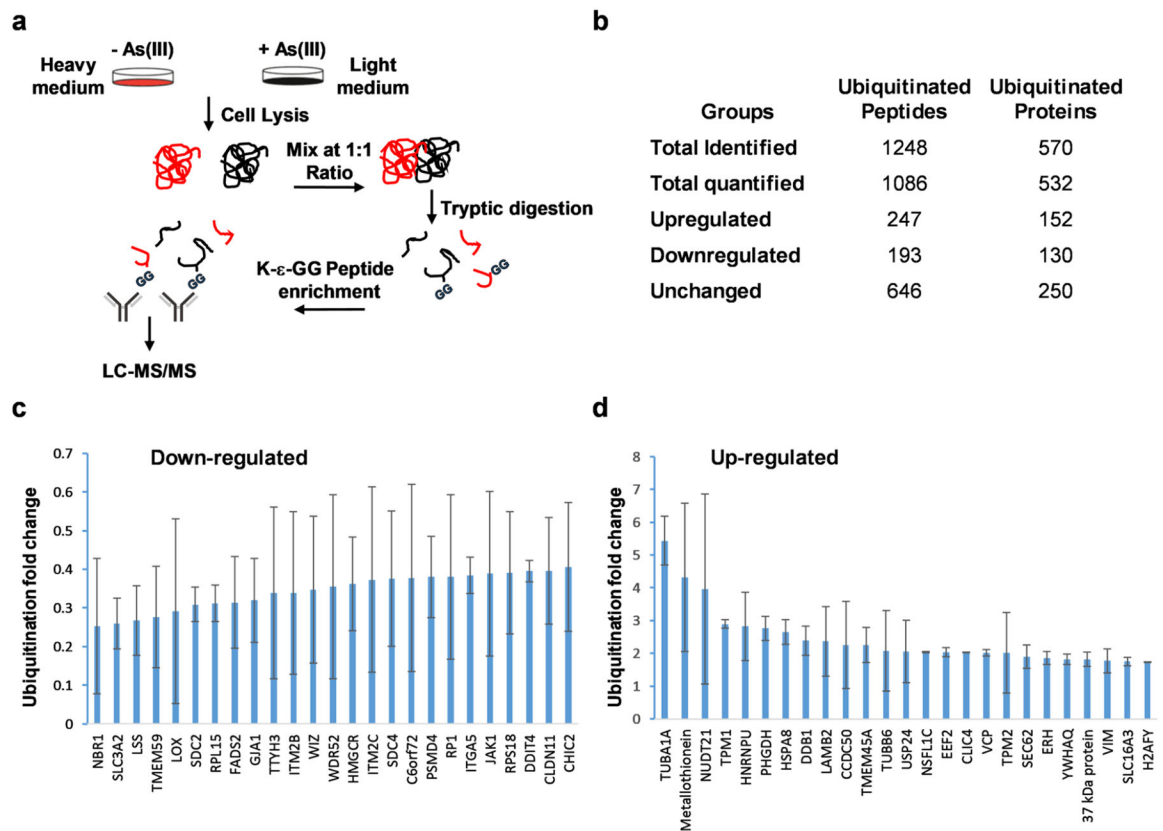


**Figure 1.** Quantitative assessment of arsenite-induced alterations in ubiquitination of the entire human proteome. (a) Workflow involves metabolic labeling using SILAC, tryptic digestion, affinity enrichment of K- $\epsilon$ -GG-bearing peptides, and LC-MS and MS/MS for the identification and quantification of ubiquitination levels. (b) Summary of identified and quantified ubiquitinated peptides and proteins. (c, d) Bar graphs showing the mean  $\pm$  SD of fold changes of 25 proteins with the most pronounced decreases (c) and increases (d) in ubiquitination levels after arsenite treatment.

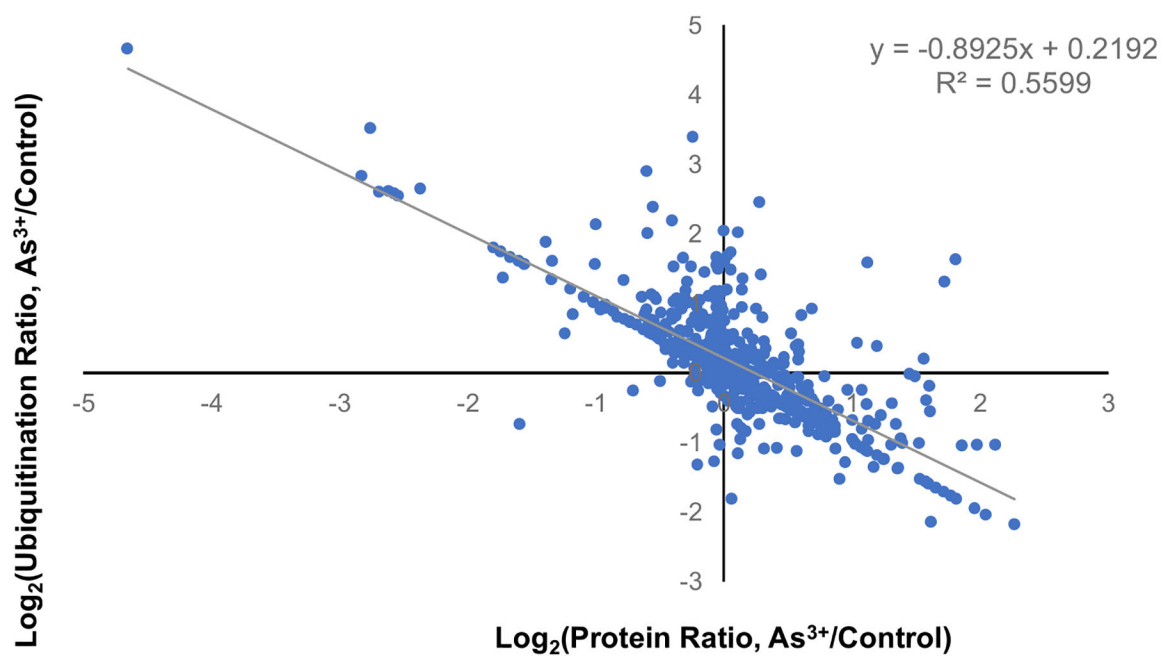


**Figure 2.** Plot showing the correlation between the  $\text{log}_2(\text{Ratio})$  of the ubiquitination levels of proteins and  $\text{log}_2(\text{Ratio})$  of the expression levels of the same proteins.

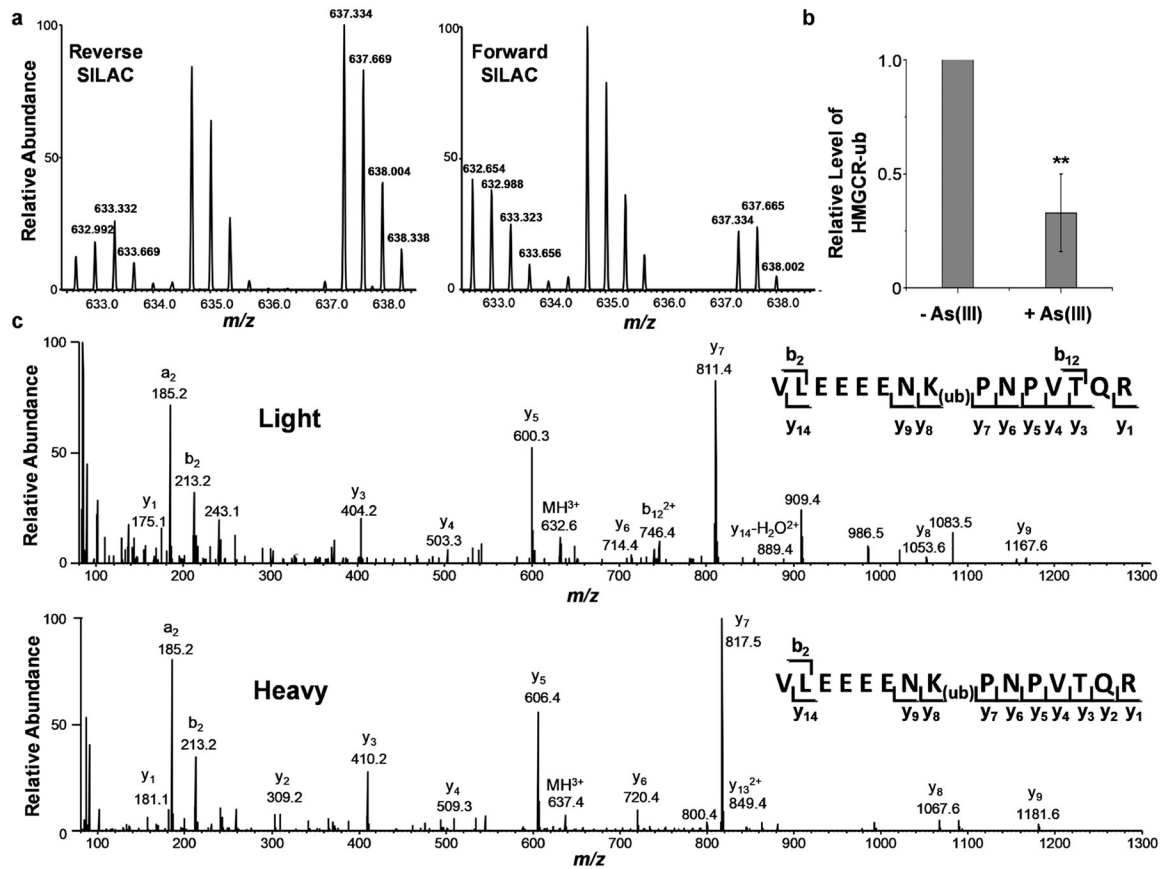


**Figure 3.**

(a) Full-scan ESI-MS showing the  $[M + 3H]^{3+}$  ions of the K248- $\epsilon$ -GG-containing peptide from HMGCR in forward and reverse SILAC experiments. (b) Quantitative analysis of arsenite-induced diminution in HMGCR ubiquitination. The  $p$  value was calculated using two-tailed unpaired Student's  $t$ -test ( $n = 3$ ): \*\*,  $0.001 < p < 0.01$ . (c) MS/MS of the light and heavy K248- $\epsilon$ -GG-carrying peptides derived from HMGCR.



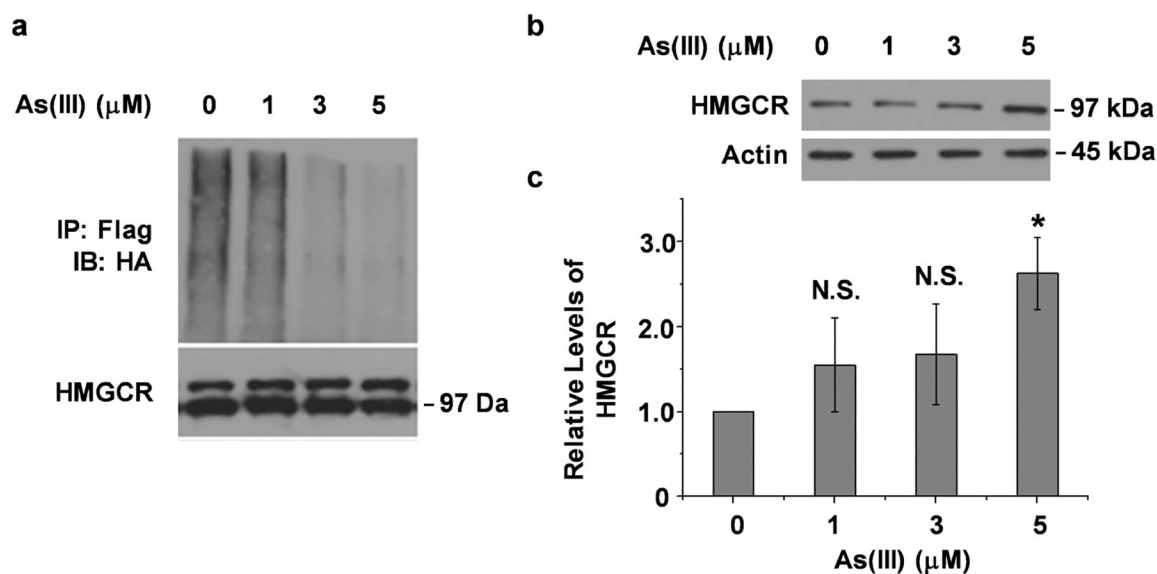


**Figure 4.**

Arsenite stabilizes HMGCR by inhibiting its ubiquitination. (a) HEK293T cells were transfected with HMGCR-Flag and HA-ubiquitin and subsequently treated with increasing doses of arsenite. The whole-cell lysates were immunoprecipitated with anti-Flag M2 magnetic beads and blotted with an anti-HA primary antibody. The result showed a decreased ubiquitination level of HMGCR upon arsenite treatment. (b) HEK293T cells were treated with increasing doses of arsenite and blotted with an anti-HMGCR primary antibody. The result revealed an increased HMGCR protein level upon arsenite treatment. (c) Quantification of the HMGCR protein level upon arsenite treatment. The  $p$  value was calculated using two-tailed unpaired Student's  $t$ -test ( $n = 3$ ): \*,  $0.01 < p < 0.05$ . "NS" represents not significant ( $p > 0.05$ ).

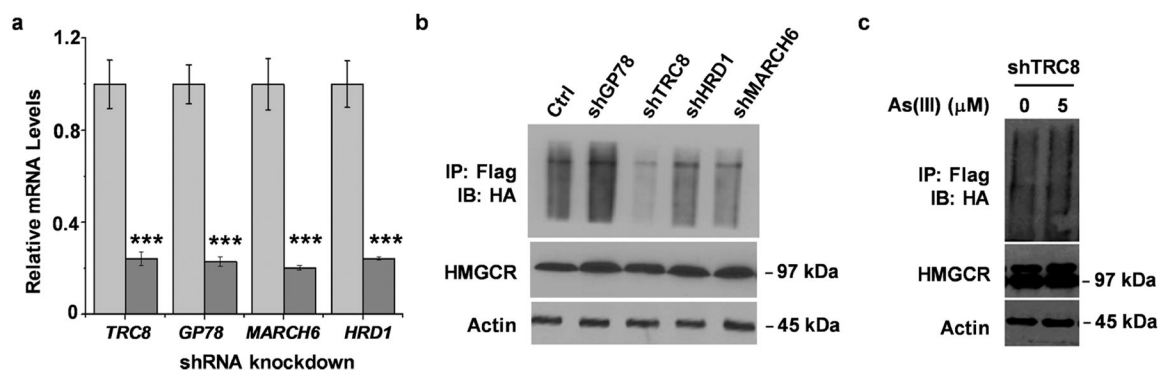


**Figure 5.**

$As^{3+}$  suppresses the ubiquitination of HMGCR in HEK293T cells through TRC8. (a) Knockdown efficiencies of shRNAs targeting *TRC8*, *GP78*, *MARCH6*, and *HRD1* genes. The  $p$  value was calculated by using two-tailed unpaired Student's  $t$ -test ( $n = 3$ ): \*\*\*,  $p < 0.001$ . (b) Knockdown of TRC8, but not GP78, MARCH6, or HRD1, gave rise to decreased HMGCR ubiquitination. HEK293T cells were transfected with HMGCR-Flag and HA-ubiquitin and subsequently transfected with shRNAs targeting the *TRC8*, *GP78*, *MARCH6*, or *HRD1* gene. The whole-cell lysate was immunoprecipitated with anti-Flag M2 magnetic beads and blotted with an anti-HA primary antibody. (c) Knockdown of TRC8 abolished the arsenite-induced decrease in HMGCR ubiquitination. HEK293T cells were transfected with HMGCR-Flag and HA-ubiquitin and subsequently transfected with shTRC8 and treated with sodium arsenite. The whole-cell lysate was immunoprecipitated with anti-Flag M2 magnetic beads and blotted with an anti-HA primary antibody.

**Table 1.**

KEGG Pathway and Functional Category Analyses Revealed the Role of Arsenite in Decreasing Ubiquitination of Proteins Involved in Different Cellular Pathways<sup>a</sup>

functional categories	no. of genes	functional categories	no. of genes
ribosome	14	proteasome	7
vibrio cholerae infection	5	neurotrophin signaling pathway	11
steroid biosynthesis	6	viral myocarditis	8
bilateral cardiomyopathy	11	pathogenic <i>Escherichia coli</i> infection	7
systemic lupus erythematosus	11	endocytosis	12
leukocyte transendothelial migration	12	adherens junction	7
ECM-receptor interaction	10	regulation of actin cytoskeleton	13
hypertrophic cardiomyopathy	10	cell adhesion molecules	9
focal adhesion	16	tight junction	12

<sup>a</sup>The protein IDs of 136 proteins in which the ubiquitinated peptides were down-regulated by at least 1.5-fold upon arsenite treatment were submitted into the DAVID bioinformatics resources 6.7 database (<https://david.ncifcrf.gov/>) for KEGG pathway analysis. The results revealed the role of arsenite in regulating key cellular pathways by inhibiting protein ubiquitination, including the sterol biosynthesis pathway.

**Table 2.**

List of Proteins Involved in the Cholesterol Biosynthesis Pathway, including HMGCR, That are with Altered Levels of Ubiquitination in GM00637 Cells Following a 24 h Exposure to 5.0  $\mu$ M Arsenite<sup>a</sup>

protein name	ubiquitination site(s)	fold changes (mean $\pm$ SD)
24-dehydrocholesterol reductase (DHCR24)	VRDIQ <b>K</b> QVR	0.58 $\pm$ 0.01
	E <b>K</b> LGCQDAFPEVYDK	0.62 $\pm$ 0.09
	ISLL <b>K</b> LTQGETLR	0.66 $\pm$ 0.10
7-dehydrocholesterol reductase (DHCR7)	KP <b>K</b> VIECSYTSADGQR	0.49
	LSDIWA <b>K</b> TPPITR	0.63 $\pm$ 0.15
3-hydroxy-3-methylglutaryl-coenzyme A reductase (HMGCR)	VLEEEEN <b>K</b> PNPVTQR	0.30 $\pm$ 0.13
	VSLGLDENV <b>S</b> KR	0.42 $\pm$ 0.18
farnesyl-diphosphate farnesyltransferase 1 (FDFT1)	IPDSDPSS <b>S</b> KTR	0.51
	ANSMGLFLQ <b>K</b> TNIIR	0.63
lanosterol synthase (LSS)	LSQVPDNPDPYQ <b>K</b> YYR	0.33 $\pm$ 0.18
	NPDGGFATYET <b>K</b> R	0.51 $\pm$ 0.16
sterol-C4-methyl oxidase-like isoform 2 (SC4MOL)	IFGTDSQYNAYNE <b>K</b> R	0.59 $\pm$ 0.16

<sup>a</sup>The ubiquitination lysine sites are shown in underlined bold font. The detailed ratios obtained from Individual SILAC Experiments are Listed in Table S2.